

## On the structure and dynamics of water associated with single-supported zwitterionic and anionic membranes

A. Miskowiec, Z. N. Buck, F. Y. Hansen, H. Kaiser, H. Taub, M. Tyagi, S. O. Diallo, E. Mamontov, and K. W. Herwig

Citation: *The Journal of Chemical Physics* **146**, 125102 (2017); doi: 10.1063/1.4978677

View online: <http://dx.doi.org/10.1063/1.4978677>

View Table of Contents: <http://aip.scitation.org/toc/jcp/146/12>

Published by the [American Institute of Physics](#)

---

### Articles you may be interested in

[Modeling micelle formation and interfacial properties with iSAFT classical density functional theory](#)  
**146**, 124705124705 (2017); 10.1063/1.4978503

[Collective hydration dynamics in some amino acid solutions: A combined GHz-THz spectroscopic study](#)  
**146**, 125101125101 (2017); 10.1063/1.4978900

[A refined polarizable water model for the coarse-grained MARTINI force field with long-range electrostatic interactions](#)

*The Journal of Chemical Physics* **146**, 054501 (2017); 10.1063/1.4974833

[Computer simulations of the diffusion of Na<sup>+</sup> and Cl<sup>-</sup> ions across POPC lipid bilayer membranes](#)  
**146**, 105101105101 (2017); 10.1063/1.4977703

[Wetting at the nanoscale: A molecular dynamics study](#)

*The Journal of Chemical Physics* **146**, 114704 (2017); 10.1063/1.4978497

[Polymer dynamics under cylindrical confinement featuring a locally repulsive surface: A quasielastic neutron scattering study](#)

*The Journal of Chemical Physics* **146**, 203306 (2017); 10.1063/1.4974836

---



**COMPLETELY  
REDESIGNED!**

**PHYSICS  
TODAY**

*Physics Today* Buyer's Guide  
Search with a purpose.

# On the structure and dynamics of water associated with single-supported zwitterionic and anionic membranes

A. Miskowiec,<sup>1</sup> Z. N. Buck,<sup>1</sup> F. Y. Hansen,<sup>2</sup> H. Kaiser,<sup>1</sup> H. Taub,<sup>1,a)</sup> M. Tyagi,<sup>3,4</sup> S. O. Diallo,<sup>5</sup> E. Mamontov,<sup>5</sup> and K. W. Herwig<sup>5</sup>

<sup>1</sup>*Department of Physics and Astronomy and University of Missouri Research Reactor, University of Missouri, Columbia, Missouri 65211, USA*

<sup>2</sup>*Department of Chemistry, Technical University of Denmark, IK 207 DTU, DK-2800 Lyngby, Denmark*

<sup>3</sup>*Center for Neutron Research, National Institute of Standards and Technology, Gaithersburg, Maryland 20899-6102, USA*

<sup>4</sup>*Department of Materials Science and Engineering, University of Maryland, College Park, Maryland 20742, USA*

<sup>5</sup>*Spallation Neutron Source, Oak Ridge National Laboratory, Oak Ridge, Tennessee 37831, USA*

(Received 6 October 2016; accepted 1 March 2017; published online 29 March 2017)

We have used high-resolution quasielastic neutron scattering (QENS) to investigate the dynamics of water molecules (time scale of motion  $\sim 10^{-11} - 10^{-9}$  s) in proximity to single-supported bilayers of the zwitterionic lipid DMPC (1,2-dimyristoyl-sn-glycero-3-phosphorylcholine) and the anionic lipid DMPG (1,2-dimyristoyl-sn-glycero-3-phosphoglycerol) in the temperature range 160–295 K. For both membranes, the temperature dependence of the intensity of neutrons scattered elastically and incoherently from these samples indicates a series of freezing/melting transitions of the membrane-associated water, which have not been observed in previous studies of multilayer membranes. We interpret these successive phase transitions as evidence of different types of water that are common to the two membranes and which are defined by their local environment: bulk-like water located furthest from the membrane and two types of confined water in closer proximity to the lipids. Specifically, we propose a water type termed “confined 2” located within and just above the lipid head groups of the membrane and confined 1 water that lies between the bulk-like and confined 2 water. Confined 1 water is only present at temperatures below the freezing point of bulk-like water. We then go on to determine the temperature dependence of the translational diffusion coefficient of the water associated with single-supported DMPG membranes containing two different amounts of water as we have previously done for DMPC. To our knowledge, there have been no previous studies comparing the dynamics of water in proximity to zwitterionic and anionic membranes. Our analysis of the water dynamics of the DMPG and DMPC membranes supports the classification of water types that we have inferred from their freezing/melting behavior. However, just as we observe large differences in the freezing/melting behavior between these model membranes for the same water type, our measurements demonstrate variation between these membranes in the dynamics of their associated water over a wide temperature range. In particular, there are differences in the diffusive motion of water closest to the lipid head groups. Previously, QENS spectra of the DMPC membranes have revealed the motion of water bound to the lipid head groups. For the DMPG membrane, we have found some evidence of such bound water molecules; but the signal is too weak for a quantitative analysis. However, we observe confined 2 water in the DMPG membrane to undergo slow translational diffusion in the head group region, which was unobserved for DMPC. The weak temperature dependence of its translational diffusion coefficient allows extrapolation to physiological temperatures for comparison with molecular dynamics simulations. *Published by AIP Publishing.* [<http://dx.doi.org/10.1063/1.4978677>]

## I. INTRODUCTION

The functioning of bilayer lipid membranes that bound living cells depends intimately on the location, structure, and motion of their associated water. Thus, there has been a strong motivation to study the dynamics of the hydration water at the molecular level in model systems such as bare

bilayer membranes (without inserted proteins) by quasielastic neutron scattering (QENS). For over 25 years, QENS has provided an important complement to other techniques such as NMR by probing the water dynamics at time scales in the  $10^{-9}$ – $10^{-13}$  s range.<sup>1–7</sup> For example, the wave vector ( $Q$ ) dependence of QENS inaccessible to NMR can be used to infer the length scale of the water motion and to distinguish between different types of translational and rotational motion.

In order to achieve adequate counting rates, most previous QENS investigations of the dynamics of membrane-associated

<sup>a)</sup> Author to whom correspondence should be addressed. Electronic mail: [taubh@missouri.edu](mailto:taubh@missouri.edu)

water have used multilamellar systems consisting of stacks of a thousand or more membranes supported on a solid substrate.<sup>1–7</sup> Unfortunately, the complexity of these samples renders them difficult to model by molecular dynamics (MD) simulations and to characterize by Atomic Force Microscopy (AFM). The sheer number of membranes, the interactions between the membranes in a stack, and the presence of unknown amounts of water between the membranes render modeling of their water dynamics by computer simulation virtually impossible.

In the absence of simulations, QENS measurements on multilayer stacks of membranes have generally been interpreted assuming just two types of water, bulk-like and membrane-bound, and their dynamics analyzed with simple analytical models of rotation and translation. For example, König *et al.*<sup>1</sup> used QENS measurements on a picosecond time scale to investigate multilayers of DPPC. They found evidence of rotational motion of tightly bound water at a low level of hydration and a temperature of 328 K with additional translational diffusion occurring at higher hydration at 317 K. Swenson *et al.*<sup>5</sup> performed QENS measurements on fully hydrated multilayers of DMPC. They report evidence of rotational motion of water at 260 K on a time scale of 100 ps with the onset of translational motion at 290 K, slightly below the gel-to-fluid transition.

As an alternative to measurements on multilamellar samples, we have recently reported QENS investigations of the water dynamics of well-characterized *single* lipid bilayers supported on an SiO<sub>2</sub>-coated silicon substrate. Both a charge-neutral zwitterionic membrane DMPC (1,2-dimyristoyl-sn-glycero-3-phosphorylcholine)<sup>8,9</sup> and an anionic membrane DMPG (1,2-dimyristoyl-sn-glycero-3-phosphoglycerol)<sup>9</sup> have been studied. A schematic diagram of the samples used is shown in Fig. 1(a). Both the DMPC and DMPG lipids contain two aliphatic chains of 14 carbon atoms and differ only in the terminal subunit of their head group: a positive choline group (zwitterionic DMPC) and a neutral glycerol (anionic DMPG). For this reason, these samples offer the interesting possibility of investigating the effect of the different structure and electric charge of their head groups on the water dynamics.<sup>9</sup>

There have been several recent MD simulations that have investigated the structure and dynamics of water hydrating single freestanding bilayers.<sup>10–14</sup> In particular, simulations of freestanding DMPC<sup>10</sup> and DMPG<sup>14</sup> membranes have proved to be of some value in interpreting our QENS measurements on single-supported membranes,<sup>8,9</sup> although one must be cautious in their use due to the possible effects of the substrate as we discuss below.

We have found that the high homogeneity and relative simplicity of the single-supported membrane samples, which can be confirmed by AFM, result in a distinctive freezing/melting behavior of their associated water,<sup>8,9</sup> which has not been observed in QENS studies of multilamellar samples.<sup>1,4,5</sup> Based on the temperature dependence of the intensity of neutrons scattered elastically and incoherently from samples with various amounts of water, we propose four different water types that are common to the zwitterionic and anionic membranes and presumably occupy different local environments:

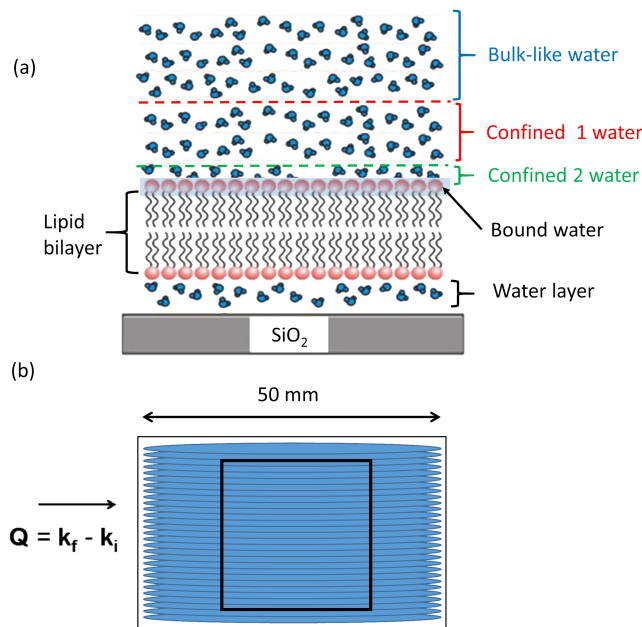


FIG. 1. (a) Sketch of a hydrated single-supported bilayer membrane as adapted from Ref. 9. Water types inferred for the DMPG and DMPC membranes from the freezing/melting behavior of their associated water and the analysis of their QENS spectra are indicated schematically: bulk-like, confined 1 and 2, and bound. (b) Schematic diagram of the neutron scattering sample consisting of a stack of Si(100) wafers, indicating the direction of the neutron wave vector transfer  $\mathbf{Q} = \mathbf{k}_f - \mathbf{k}_i$  with respect to the wafer plane. The square outline indicates the size of the neutron beam incident on the sample.

bulk-like water located furthest above the membrane, two types of confined water in closer proximity to the lipid head groups,<sup>8,9</sup> and water bound to the head groups as indicated schematically in Fig. 1(a). A water type termed “confined 2” is located within and just above the lipid head groups of the membrane and confined 1 water lies between the frozen bulk-like and confined 2 water.

In this paper, we extend our study by determining the temperature dependence of the translational diffusion coefficient of the water associated with single-supported DMPG membranes containing two different amounts of water as we have previously done for DMPC.<sup>9</sup> To our knowledge, there are no previous studies comparing the dynamics of water in proximity to zwitterionic and anionic membranes. The QENS studies in Refs. 1–7 have been confined to PC membranes and have not probed the translational diffusion of the membrane-associated water below room temperature. Our analysis of the water dynamics of the DMPG and DMPC membranes supports the classification of water types that we have inferred from their freezing/melting behavior. However, just as we observe large differences in the freezing/melting behavior between these model zwitterionic and anionic membranes for the same water type, our measurements demonstrate variation between these membranes in the dynamics of their associated water over a wide temperature range. In particular, there are differences in the diffusive motion of water closest to the lipid head groups. For DMPG, we show that the translational diffusion coefficient of confined 2 water is weakly temperature dependent, allowing extrapolation of our values to physiological temperatures for comparison with MD simulations.

## II. METHODS

### A. Sample preparation and water content

As described previously, we deposited the single-supported DMPC membranes by a vesicle fusion process.<sup>8,9,15</sup> The substrate consisted of a cylindrical stack of about 100 acid-cleaned, electronic-grade Si(100) wafers (5 cm diameter, 0.3 mm thick, and polished on both sides) as shown in Fig. 1(b).<sup>16</sup> DMPC ( $C_{36}H_{72}NO_8P$ ) from Avanti Polar Lipids<sup>17</sup> at a concentration of 1.5 mg/ml was added to a solution of 100 mM KCl ( $M = \text{mol/l}$ ), 5 mM  $MgCl_2$ , and 5 mM HEPES ( $C_8H_{18}N_2O_4S$ ) and sonicated at 318 K for  $\sim 24$  h to produce multilamellar vesicles of micron size as confirmed by dynamic light scattering. After the deposition of DMPC for 1 h at 328 K, the wafers were rinsed in distilled water to remove additional membrane layers and salt and then dried in  $N_2$  gas. The wafer stack was loaded into an aluminum cell sealed with an indium O-ring under a helium atmosphere. Although not precisely controlled, the water content of the membranes could be varied by first annealing the samples in an oven at 328 K for 3 days prior to loading them in the aluminum sample cell and then rehydrating them by introducing a water droplet into the sample can before sealing, a procedure followed for the “wet” DMPC and DMPG samples as discussed below. The “dry” DMPG sample did not undergo a 3-day annealing and no water droplet was added to it.

We have found deposition by vesicle fusion of large, homogeneous, single-supported DMPG ( $C_{34}H_{66}O_{10}P$ ) membranes to be more difficult than for DMPC principally due to the sensitivity to the divalent salt concentration. Previous AFM studies of PG membranes have used smaller samples of POPG deposited on a mica substrate by the Langmuir-Blodgett technique.<sup>18</sup> Our preparation of the sodium salt of DMPG as provided by Avanti Polar Lipids<sup>17</sup> began by suspending the lipid powder in a chloroform:methanol:water solution in a glass vial with fluid volumes in the ratio 65:35:8 (the same ratio as for DMPC). The solution was allowed to evaporate under a gentle stream of nitrogen gas, resulting in a thin film of lipid material uniformly deposited on the inner walls of the vial. We then rehydrated the powder solution with 15 mM KCl (a lower concentration than for DMPC) and 15 mM  $MgCl_2$ . A higher concentration of  $MgCl_2$  than for the deposition of single membranes of DMPC was required in order to facilitate the formation of planar membrane structures.<sup>19</sup> The solution was then heated to 318 K and sonicated for  $\sim 24$  h to break up larger aggregates before filtering through a 100 nm filter in a LiposFast apparatus also from Avanti.<sup>17</sup> The resultant solution was clear and contained small, mostly unilamellar vesicles.

The DMPG solution was then diluted to a concentration of 15  $\mu\text{g/ml}$ . Silicon wafers were immersed in the solution and incubated for 1 h at 338 K during which time the vesicle fusion occurred. Upon removal, water appeared to wet the wafer, in contrast to wafers with deposited DMPC, and the remaining buffer solution was allowed to evaporate in air. Because the membrane is so weakly bound to the substrate, the salt solution cannot be rinsed away as in the DMPC preparation.

As shown in Fig. S2 (in the [supplementary material](#)), topographic images recorded by AFM from similarly prepared samples under a flow of moist air showed homogeneous

DMPC and DMPG membranes of comparable quality with few holes or cracks.<sup>19,20</sup> The membranes had a typical thickness of  $\sim 6.3$  nm at room temperature, which is somewhat larger than the  $\sim 4.6$  nm reported from neutron reflectivity measurements on single-supported DMPC membranes submerged in  $D_2O$ .<sup>21</sup> Possible reasons for this discrepancy include the thickness of the water layer between the lower leaflet and the  $SiO_2$  surface and the out-of-plane disorder of the lipid molecules as discussed in Ref. 8. The temperature dependence of the membrane thickness measured by AFM indicated that below 328 K both the DMPC and DMPG bilayers were in their gel phase.<sup>19,20</sup> Presumably, the interaction of the membrane’s proximal leaflet with the  $SiO_2$  surface and a relatively low level of hydration favor an area per lipid close to that of the gel phase. Molecular dynamics simulations are in progress to determine the effect of the  $SiO_2$  substrate on the bilayer properties.

The water content of our samples was determined as follows. The so-called “wet” samples were prepared by first annealing in air for 72 h at a temperature of 328 K before sealing the wafer stack in an Al sample can with 120  $\mu\text{l}$  of  $H_2O$ . This amount of water is substantially greater than that required to hydrate the membranes completely.

As discussed previously,<sup>8,9,19</sup> we have used the temperature dependence of the elastic intensity to determine the total number of H atoms in the water and lipid molecules of our membrane samples (see Fig. 2). The increase in intensity from high temperature ( $T > 328$  K) to low temperature [ $T < 245$  K (DMPC) and  $T < 200$  K (DMPG)] is attributed to the freezing of water and lipids because at high temperatures the H atoms in these components are moving faster than the time scale of

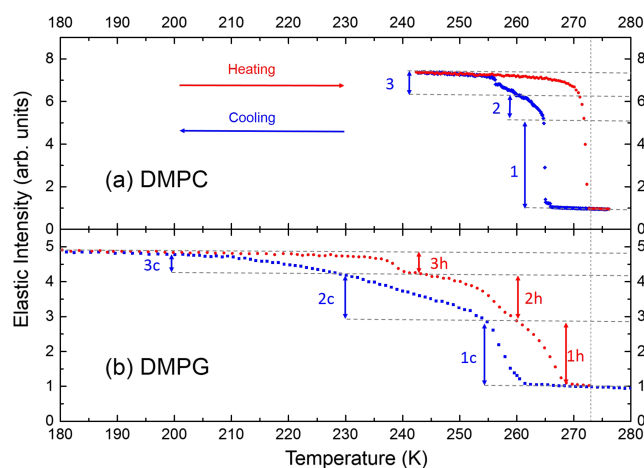


FIG. 2. Comparison of the incoherent elastic neutron intensity as a function of temperature for single-supported membranes with water in excess of full hydration (denoted “wet”) as measured on the backscattering spectrometer HFBS at NIST: (a) DMPC and (b) DMPG. The intensity has been summed over all wave vector transfers and normalized to unity at  $T = 270$  K. The blue and red data points were taken on cooling (0.04 K/min) and heating (0.1 K/min), respectively. Temperature sensors placed on the top and bottom of the sample cell indicated thermal equilibrium during the cooling and heating cycles. The vertical double arrows indicate the intensity increment (decrement) associated with freezing (melting) of each water type (labeled with subscripts 1–3). For DMPG, the labels “c” and “h” on the arrows indicate cooling and heating, respectively, numbered substeps in its heating curve match intensity increments in its cooling curve. For DMPC, the location of the freezing transition labeled “2” was determined from the temperature dependence of the diffusion coefficient in Fig. 8. Adapted from Ref. 9.

the high-flux backscattering spectrometer (HFBS); and, at the low-temperature limit, these H atoms are immobilized. This intensity increase can be calibrated against that produced by a known number of H atoms in an alkane film deposited on an identical silicon substrate,<sup>16</sup> yielding the total number of H atoms in the water and lipid molecules of our membrane samples.

We estimate the number of lipid molecules by assuming that each side of the Si wafers is completely covered by a single bilayer as is consistent with our AFM images (see Fig. S2 of the [supplementary material](#)). Knowing the total surface area of the wafers and the area per lipid in the gel phase from Ref. 14 (56 Å<sup>2</sup> and 47 Å<sup>2</sup> for the DMPC and DMPG membranes, respectively), we can compute the number of lipids in the sample. In this way, we estimate the lipid molecules to contain ~3% (DMPC) and ~6% (DMPG) of the total number of H atoms in the samples.

We then compute the number of H atoms in the membrane-associated water from the total number of H atoms minus the number in the lipids. Assuming it to have the bulk density, we infer the water in the wet DMPC and DMPG samples in Fig. 2 to be equivalent to a slab on each side of a wafer of thickness ~110 nm and ~71 nm, respectively. We emphasize that the morphology of the water is unknown, i.e., whether the liquid is in the form of droplets or wets the membrane as a slab of uniform thickness.<sup>8</sup> These effective water thicknesses correspond to ~1060 and ~560 water molecules per lipid in our wet DMPC and DMPG samples, respectively, assuming the bilayer membranes to be in their gel phase.<sup>19,20</sup> X-ray measurements give 27 water molecules per lipid required for complete hydration of DMPC<sup>22</sup> in good agreement with a value of 28 from our MD simulations.<sup>10</sup> For a freestanding DMPG membrane, our simulations give 10 and 18 water molecules per lipid, for the gel and fluid phases, respectively.<sup>14</sup>

### B. Quasielastic and elastic neutron scattering

The QENS measurements were performed on the backscattering spectrometer BASIS<sup>23</sup> at the Spallation Neutron Source (SNS), Oak Ridge National Laboratory and the High-Flux Backscattering Spectrometer (HFBS)<sup>24</sup> at the Center for Neutron Research, National Institute of Standards and Technology (NIST NCNR). BASIS has an energy resolution width at zero energy transfer of  $\Delta E \sim 3.5 \mu\text{eV}$ , allowing motions on a time scale of ~1 ns and faster to be probed. The largest energy transfer accessible (dynamic range) is  $\pm 120 \mu\text{eV}$ , corresponding to a time scale down to ~30 ps. The energy resolution of the HFBS is  $\Delta E \sim 1 \mu\text{eV}$ , yielding a time scale of ~4 ns, which is somewhat better than BASIS; but it comes with a smaller dynamic range, which in our measurements is limited to  $\pm 17 \mu\text{eV}$ .

The HFBS can be operated in a stationary monochromator mode to measure the elastically scattered neutron intensity (neutrons scattered with an energy transfer less than the energy width of the resolution function  $\Delta E$ ). We refer to scans of the elastic intensity vs. temperature as Fixed Window Scans (FWS). The slowest temperature ramp rate possible in our measurements was 0.04 K/min.

We note that using our relatively large samples, FWS provide a sensitivity to water freezing transitions that is

inaccessible to differential scanning calorimetry (DSC) with commercially available instruments. Scaling the water content of our 100-wafer neutron scattering sample (~120 μl) by the surface area of wafers that would fit in the sample volume of a commercial DSC apparatus yields a water content of ~0.06 μl or one to two orders of magnitude less water than typically required to detect freezing transitions.

## III. RESULTS

### A. Elastic neutron scans

The elastic intensity (HFBS monochromator stationary) was recorded on both slow cooling of the sample (0.04 K/min, blue points) and on heating (0.1 K/min, red points) in Figs. 2 and 3. It has been summed over all wave vector transfers to increase the intensity and measures the number of neutrons scattered with energy transfers less than ~1 μeV, the full width at half maximum (FWHM) of the HFBS resolution function. Because incoherent scattering from the hydrogen atoms dominates the elastic signal, an increase in the elastic intensity is proportional to a decrease in the number of H atoms in the sample moving at a time scale faster than ~4 ns.

In Fig. 2, we compare the temperature dependence of the intensity of incoherently elastically scattered neutrons from wet samples of single-supported DMPC and DMPG membranes<sup>8,9</sup> as measured on the HFBS at the NIST NCNR.<sup>24</sup> In the temperature range 273 K <  $T$  < 328 K where the supported DMPC and DMPG bilayers are in the gel phase and the motion of H atoms in the water molecules is faster than the time scale of the instrument, the elastic scattering is dominated by a temperature-independent contribution from the silicon substrate (~70%) with a smaller contribution from the H atoms in the lipid membrane (~30%). These fractions are determined

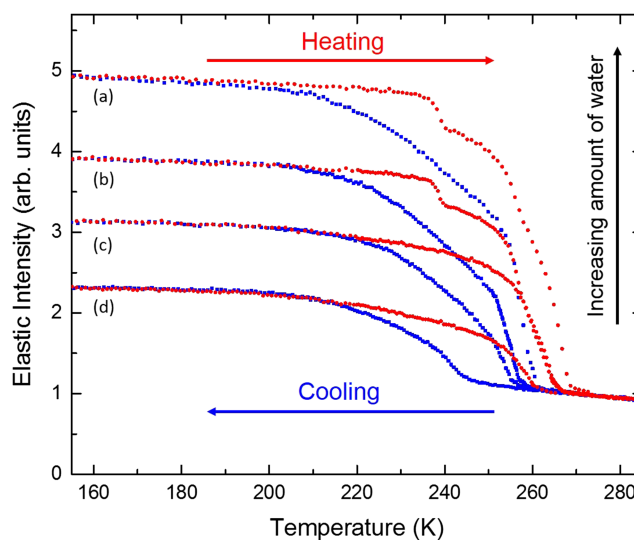


FIG. 3. Elastic scans measured on the HFBS for DMPG samples having four different amounts of water from Ref. 9. The corresponding equivalent water thicknesses (see text for definition) are (a) 71 nm; (b) 52 nm; (c) 39 nm; and (d) 23 nm. The data have been summed over all wave vector transfers and normalized to unity at  $T = 270$  K. The blue and red data points were taken on cooling (0.04 K/min) and heating (0.1 K/min), respectively. To facilitate comparison of the wet DMPG sample in (b) with the samples of lower amounts of water, we have included its elastic scan labeled (a).

by the number of silicon atoms in the substrate, the number of lipid H atoms, and their incoherent neutron cross sections. The lipid-H contribution to the elastic intensity decreases slightly as the temperature increases in this range due to the broadened gel-to-fluid transition of the supported DMPC and DMPG membranes.<sup>19,20</sup>

In Fig. 2(a), we see that a wet DMPC membrane exhibits a temperature dependence of the elastic intensity significantly different from that of the wet DMPG sample [Fig. 2(b)] both on heating and cooling. The two samples differ in their melting as well as their freezing behavior. On heating, the DMPC membrane shows a relatively abrupt decrease in its elastic intensity close to the bulk water melting point of 273 K [see Fig. 2(a)]. There is only a small pre-melting effect beginning near 267 K as indicated by a more rapid intensity decrease. On the other hand, the DMPG membrane has a more gradual decrease in the intensity on heating. We see in Fig. 2(b) that there is a downward substep near 237 K followed by weaker and broader substeps near 242 K and 260 K, respectively, with the intensity leveling off at  $\sim 269$  K, i.e., below the melting point of bulk ice.

On cooling, freezing of water for the DMPG membrane occurs over a larger temperature range  $\Delta T_F \sim 70$  K than for DMPC ( $\Delta T_F \sim 10$  K). Here we are measuring the transition widths as the difference between the temperature at which the heating and cooling curves merge ( $\sim 256$  K for DMPC and  $\sim 200$  K for DMPG) and the temperature at which the initial rise in the elastic intensity (freezing) occurs. The wet DMPC sample displays a vertical step in the elastic intensity at a temperature of 265 K followed by a continuous increase in the intensity whereas the DMPG membrane shows a steep initial rise in the intensity on cooling below  $\sim 260$  K, but no vertical step, followed by a more gradual increase in the elastic intensity.

In Fig. 3, we compare the HFBS elastic scan of the wet DMPG sample in Fig. 2(b) with three other DMPG samples containing less water down to an equivalent water thickness of  $\sim 23$  nm. The three samples with the most water exhibit a qualitatively similar and reproducible temperature dependence of the elastic intensity on cooling. They differ principally in that both the onset temperature of the increase in the elastic intensity and the magnitude of its initial rise tend to decrease with a lower water content. Their similarity can be seen more clearly in Fig. 4 where we define three characteristic temperature ranges on cooling: Region 1 ( $255 \text{ K} < T < 260 \text{ K}$ ) in which the initial rapid rise in the elastic intensity occurs; Region 2 ( $230 \text{ K} < T < 250 \text{ K}$ ) in which the intensity increases more slowly and nearly linearly in temperature; and Region 3 ( $T < 230 \text{ K}$ ) over which the intensity levels off to a nearly constant value. The elastic intensity does not reach its low-temperature limit until  $\sim 200$  K. The behavior of the sample with the least amount of water [Fig. 3(d)] differs from the other three in that the initial rise in the elastic intensity occurs at a lower temperature of  $\sim 244$  K, and the transition from a nearly linear intensity increase in Region 2 to the saturating behavior in Region 3 is not as well defined (see Fig. 4). These features are probably related to the larger amount of the more localized confined 2 water relative to confined 1 water in the dry sample compared to the wet sample and the possibility of a larger salt

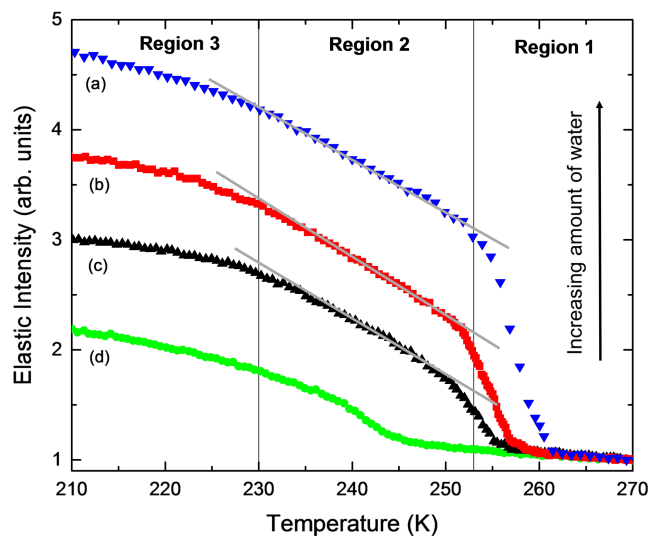


FIG. 4. A magnified version of Fig. 3 to elucidate features of the elastic scans. Three characteristic regions are seen in the figure and discussed in the text. Region 1: freezing of bulk-like water above the membrane in the three samples with the highest water content [scans (a)–(c)]. The intensity increment in Region 1 for these samples scales with the amount of water. Region 2: freezing of confined 1 water closer to the lipid head groups in the three samples with the highest water content. In Region 2, the slope of the linear intensity increase agrees within 4% for the three samples with the highest amount of water, indicating that the amount of confined 1 water freezing is independent of the total water content. Region 3: freezing of water closest to the membrane. The so-called dry sample (d), having the lowest water content, appears to have only a small amount of bulk-like and confined 1 water.

concentration in the dry sample as will be discussed in Secs. IV B and V B.

As indicated by the pairs of vertical double arrows of equal length in Fig. 2(b), there is reasonable agreement between the intensity decrement in each of the substeps on heating of the DMPG sample with the corresponding intensity increments that occur on cooling in the three temperature regions identified in Fig. 4. In particular, the intensity decrement on heating through the substep near 237 K labeled 3h agrees well with the intensity increment 3c on cooling through the more poorly defined third region,  $T < 230$  K [see Fig. 2(b)]. This consistency between the cooling and heating intensity curves tends to support the three distinct temperature ranges previously identified in the cooling scan.

On heating, we see in Fig. 3 that the two samples having the lowest water content do not show the step-like decreases in the intensity as seen at higher hydration. We also note that as the water content of the DMPG samples decreases, there is a corresponding decrease in the temperature at which the melting of their ice is complete. For the sample with the least water [Fig. 3(d)], the minimum intensity (all of the elastic scattering is contributed by the silicon and the H atoms in the lipids) occurs at  $\sim 260$  K or about 18 K below the melting point of bulk ice.

## B. Quasielastic spectra

To aid in the interpretation of our temperature scans of the elastic neutron intensity and to probe the water dynamics, we have obtained full quasielastic spectra from our two DMPG samples having the greatest difference in water content: the wet sample (equivalent water thickness of  $\sim 71$  nm) and the dry

sample (equivalent water thickness of  $\sim 23$  nm). Most of the measurements were performed on BASIS because of its larger dynamic range ( $\pm 120$   $\mu\text{eV}$ ) and only those at the lowest temperatures were also taken on the HFBS with its better energy resolution ( $\sim 1$   $\mu\text{eV}$ ). We fit the spectra using the DAVE software<sup>25</sup> by folding the instrumental resolution function with a scattering law composed of three terms: a delta function corresponding to the elastic scattering plus two Lorentzians representing the quasielastic scattering.<sup>8,9</sup> The decomposition of a BASIS spectrum into these three components and a linear background term is illustrated in Fig. 5 for the wet sample at a temperature of 253 K and  $Q = 0.9$   $\text{\AA}^{-1}$ .

As a check of the reproducibility of our elastic intensity (FWS) measurements on the HFBS, we have also measured the temperature dependence of the elastic intensity of the wet DMPG sample on BASIS, i.e., the integrated intensity of the delta-function component folded with the resolution function shown by the dashed curve (black) in Fig. 5. It agrees reasonably well with the FWS measured on the HFBS as can be seen by comparing the results in Figs. 3 and 6(a). From the BASIS spectra, we find that the increase in the delta-function intensity of the dry DMPG sample on cooling from high temperatures ( $T > 270$  K) to 230 K [Fig. 6(a)] is about a factor of 3.6 less than for the wet sample [Fig. 6(a)]. Similarly, from measurements on the HFBS [Fig. 3(d)], the increase in the elastic intensity of the dry sample over the same temperature range is about a factor of 3 less than for the wet sample. However, there is a discrepancy in the onset temperature of the steep increase in the elastic intensity on cooling, which occurs about three degrees higher (at 265 K) for the delta-function intensity. We are uncertain as to the origin of this discrepancy and cannot rule out differences in the thermometry between the sample cryostat used with the HFBS at NIST and the one used with

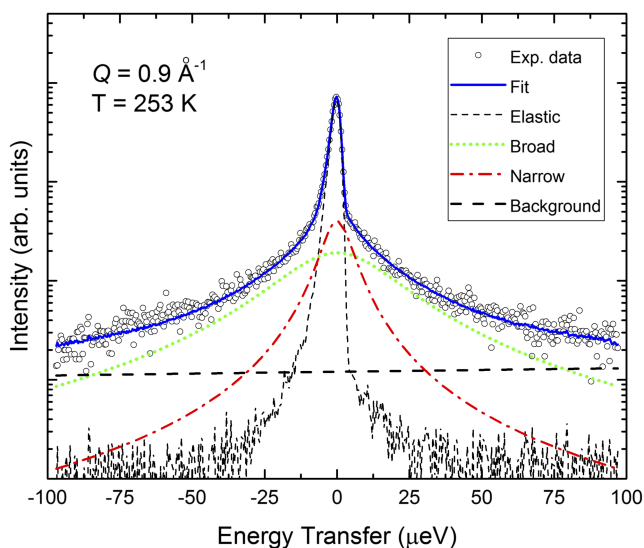


FIG. 5. The QENS spectrum of the wet DMPG sample measured on BASIS upon cooling at  $Q = 0.9$   $\text{\AA}^{-1}$  and  $T = 253$  K. The data points (open circles) have been fitted by folding the instrumental resolution function with a scattering law composed of three terms: a delta function (dashed black curve) corresponding to elastic scattering, a broad Lorentzian (green dotted curve), plus a narrow Lorentzian (red dotted-dashed curve) representing the quasielastic scattering. The best fit to the spectrum (blue solid curve) is obtained after adding a linear background term (bold dashed line).

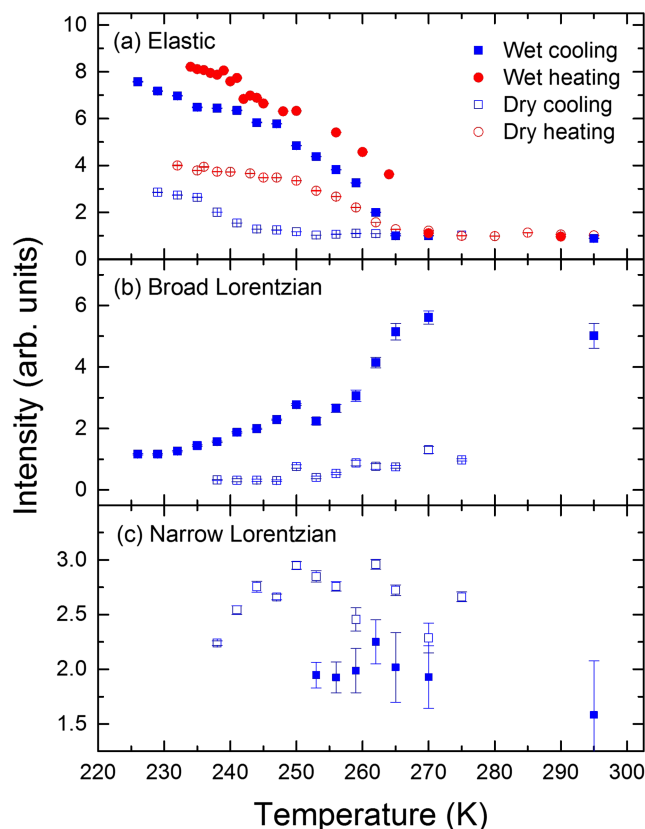


FIG. 6. Intensity of the elastic and two Lorentzian components in the QENS spectra measured on BASIS for the wet and dry DMPG samples as a function of temperature. Data for the wet and dry samples are shown with solid and open symbols, respectively. Cooling data are shown as blue squares. For clarity, heating data are shown only for the elastic intensity (red circles). (a) The elastic intensity for both the wet and dry DMPG samples averaged over all  $Q$  and normalized to unity at  $T = 270$  K. (b) The broad-Lorentzian intensity for the wet and dry samples on cooling. (c) The narrow-Lorentzian intensity for both samples on cooling. In (b) and (c), the intensity has been averaged over wave vector transfers  $Q$  of  $0.5$   $\text{\AA}^{-1}$ ,  $0.7$   $\text{\AA}^{-1}$ , and  $0.9$   $\text{\AA}^{-1}$  used in the determination of the diffusion coefficient and has been normalized to allow comparison with the elastic intensity in (a). In (a) and (b), error bars are indicated within the open symbols.

BASIS at the SNS. We also note that the measurements on BASIS were performed after storing the hermetically sealed sample at room temperature for a five-month period during which the membrane could have annealed.

### 1. High water content (wet) sample: Cooling

The large dynamic range of BASIS allows us to fit the quasielastic spectra of the wet DMPG sample with two Lorentzians in a limited range ( $253$  K  $< T < 270$  K) of the temperatures investigated ( $220$  K  $< T < 295$  K). The so-called broad and narrow Lorentzians represent motion on a “fast” and “slow” time scale, respectively. We have shown the temperature dependence of the intensity of these two Lorentzians in Figs. 6(b) and 6(c).

For the broad Lorentzian, there is a clear correlation between the drop in its intensity on cooling [Fig. 6(b)] and the rise in the elastic intensity as shown in Fig. 6(a). This correlation implies that the water molecules responsible for the broad spectral component and the rise in the elastic intensity are the same.

The intensity of the narrow-Lorentzian component in the BASIS spectra depends weakly on temperature compared to that of the broad component. This dissimilarity in the temperature dependence suggests that a different water population contributes to each, presumably a function of the position of the water molecules relative to the membrane.

Analysis of the Lorentzian components shows that the full width at half maximum (FWHM) of each has a linear dependence on  $Q^2$  at low  $Q$  characteristic of translational diffusion.<sup>10</sup> We quantify the diffusion rate of the water molecules contributing to each component by the coefficient  $D$ , which is proportional to the slope of the linear region:  $\Gamma = \text{FWHM}/2\hbar = DQ^2$ . Examples of this behavior are shown in Fig. 7, using the scattering data for the wet DMPG sample at  $T = 253$  K where the intensity of the broad- and narrow-Lorentzian components is about equal [see Figs. 6(b) and 6(c)]. At this temperature, the value of  $D$  for the water molecules contributing to the broad Lorentzian is about a factor of 5 larger than for those contributing to the narrow Lorentzian.

Figure 8 shows the temperature dependence of the diffusion coefficients for the wet DMPG sample derived from the “broad” and “narrow” Lorentzian components of the QENS spectra. For comparison, diffusion coefficients for bulk water determined from QENS<sup>26</sup> and NMR<sup>27</sup> measurements are also shown. From 270 K down to 253 K, we see that  $D$  inferred from the broad-Lorentzian component of the wet sample agrees with the values obtained for bulk supercooled water from the QENS and NMR measurements to within the experimental uncertainties. For example, at 253 K, we find  $D = 0.44 \times 10^{-5}$  cm<sup>2</sup>/s from Fig. 7(a) compared to the values  $D = 0.47 \times 10^{-5}$  cm<sup>2</sup>/s determined for bulk supercooled water by NMR<sup>27</sup> and  $D = 0.42 \times 10^{-5}$  cm<sup>2</sup>/s by QENS.<sup>26</sup> At 295 K, though, the value of  $D$  inferred from the broad-Lorentzian component is

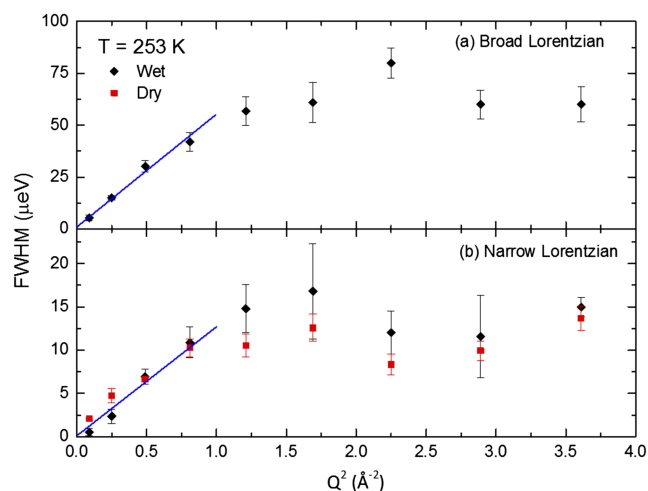


FIG. 7. FWHM as a function of  $Q^2$  for (a) the broad and (b) the narrow-Lorentzian components in the QENS spectra for the wet and dry DMPG samples at  $T = 253$  K as measured upon cooling. The slope of the blue line at low  $Q$  is proportional to the diffusion coefficient of the water component represented by each Lorentzian. In panel (a), the slope inferred from the analysis of the broad-Lorentzian component yields a diffusion coefficient close in value to that of bulk supercooled water. From panel (b), we infer the same diffusion coefficient for water in the wet and dry samples represented by the narrow-Lorentzian component and termed confined 2.

somewhat less than that of bulk water. This discrepancy may be due to the FWHM of the broad component near  $Q = 0.9 \text{ \AA}^{-1}$  becoming comparable to the dynamic range of the BASIS spectrometer ( $120 \mu\text{eV}$ ).

In addition to comparing the temperature dependence of  $D$  inferred from the broad Lorentzian component in the spectra of the wet DMPG sample with bulk supercooled water, we also compare it with that of two DMPC membranes with effective water thicknesses of  $\sim 110$  nm (wet) and  $\sim 11$  nm (dry), respectively.<sup>8</sup> At 270 K, the diffusion coefficients inferred from the broad component of the wet DMPC and DMPG samples agree to within the experimental error. This observation supports the conjecture that the broad-Lorentzian component represents the motion of bulk-like water above the membrane, which is largely unaffected by the underlying membrane.

Below 250 K, we are able to fit the QENS spectra of the wet sample with only a single Lorentzian, termed “broad” Lorentzian in Fig. 6(b). The diffusion coefficient  $D$  obtained from this fit is smaller than that for bulk supercooled water at the same temperature. We used the HFBS with its higher energy resolution to obtain spectra at the lowest temperatures where the width of the quasielastic scattering is smallest. For example, the lowest-temperature reached on cooling was 220 K (see Fig. 9) where the analysis of the HFBS spectra yielded the value  $D = 0.02 \times 10^{-5}$  cm<sup>2</sup>/s.

As noted above, we are able to fit the QENS spectra of the wet DMPG sample to two Lorentzians in the temperature range  $253 \text{ K} \lesssim T \lesssim 270 \text{ K}$ . The analysis of the narrow-Lorentzian component yields a diffusion coefficient that is both smaller and has a weaker temperature dependence than that inferred from the broad-Lorentzian component at the same temperature (see Fig. 8). Above 270 K, the narrow-Lorentzian is more difficult to resolve because its intensity is about a factor of three weaker than that of the broad component, resulting in a larger uncertainty in  $D$  at 295 K than at lower temperatures. The value of  $D$  derived from the narrow component is of primary interest because it reflects the effect of the membrane on the water dynamics. Having good data for it over a wide temperature range allows us to make a reliable extrapolation of  $D$  to physiological temperatures. Such an analysis is feasible for the dry DMPG membrane as discussed in Sec. IV D.

## 2. Low water content (dry) sample: Cooling

The dry DMPG sample is expected to have less bulk-like water; and, in fact, its broad-Lorentzian component, which we have tentatively identified with bulk-like water above the membrane, was about a factor of 5 weaker than for the wet sample at 270 K [see Fig. 6(b)]. Moreover, the dry sample’s broad-Lorentzian component had about half the intensity of its narrow-Lorentzian component [see Figs. 6(b) and 6(c)]. For this reason, we were unable to determine a translational diffusion coefficient for the bulk-like water in the dry sample.

On the other hand, it is possible to analyze the narrow-Lorentzian component in the dry sample over a wider temperature range ( $220 \text{ K} < T < 275 \text{ K}$ ) than for the wet sample (see Fig. 8). For  $T > 250$  K, its intensity is comparable to that of the wet sample [see Fig. 6(c)]; and, for  $T < 250$  K, the bulk-like

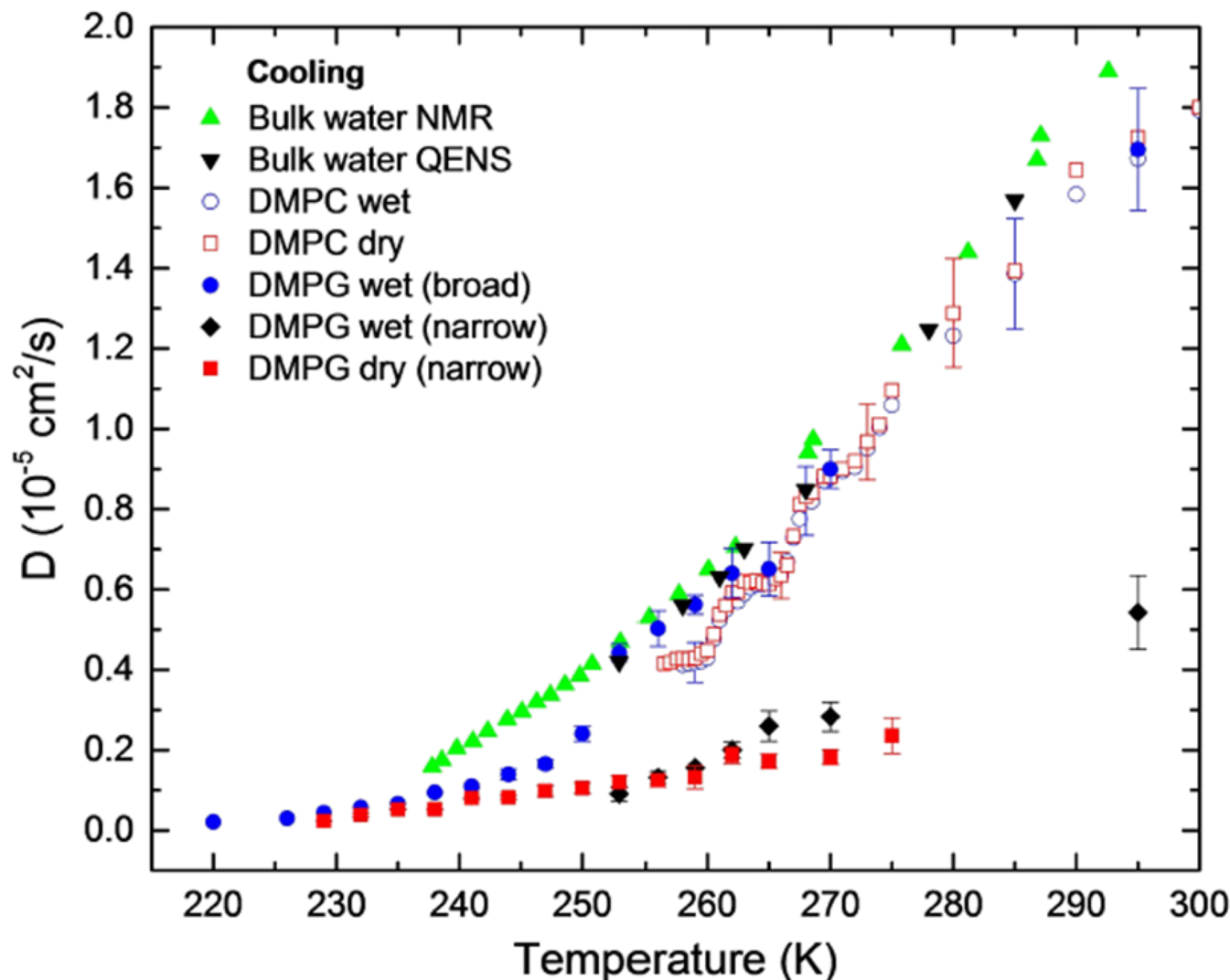


FIG. 8. Diffusion coefficients  $D$  inferred from the analysis of the QENS spectra of both wet and dry DMPG samples as a function of temperature on *cooling*. For comparison, the values of  $D$  obtained for bulk-supercooled water are also shown from NMR (green up triangles) from Ref. 27 and QENS measurements (black down triangles) from Ref. 26. The solid blue circles are obtained from the analysis of the broad-Lorentzian component of the wet sample and the black diamonds from its narrow-Lorentzian component. The solid red squares are from the analysis of the narrow-Lorentzian component of the dry sample. Also plotted are values of  $D$  for two DMPC samples with a different water content:<sup>9</sup> wet (open circles) and dry (open squares) with effective water thicknesses of  $\sim 110$  nm and  $\sim 11$  nm, respectively. The value of the diffusion coefficient of the wet DMPG at 220 K was obtained from the analysis of the QENS spectra collected on HFBS. All other diffusion coefficients for the membrane-associated water were determined from spectra collected on BASIS.

water is frozen out as discussed above so that only the narrow-Lorentzian component remains. In the restricted temperature range  $253 \text{ K} < T < 270 \text{ K}$ , where  $D$  can be determined from the analysis of the narrow-Lorentzian component in both the wet and dry samples, we find agreement in  $D$  to within the experimental uncertainty. It is evident in Fig. 8 that  $D$  inferred from the narrow-Lorentzian component is less temperature dependent than that for the broad-Lorentzian component and for bulk supercooled water. This weak temperature dependence allows a reliable extrapolation of the diffusion coefficient to physiological temperatures and comparison with our MD results, a key result.

### 3. Wet and dry samples: Heating

It was of particular interest to determine  $D$  on heating at low temperatures where we had observed a qualitative difference in the temperature dependence of the elastic intensity

between the wet and dry samples. Recall that the two samples with the most water showed a downward substep [labeled 3h in Fig. 2(a)] in the elastic intensity on heating near 237 K that was not present for the dry sample [cf. Figs. 3(a) and 3(b) with Fig. 4(d)].

Figure 9 shows the temperature dependence on heating of the diffusion coefficients determined from the analysis of the broad and narrow-Lorentzian components of the wet DMPG sample and the narrow component of the dry DMPG sample. As expected, the major difference with the diffusion coefficients obtained on cooling [see Fig. 8] occurs near 237 K [see solid and open circles in the inset of Fig. 9]. In this temperature range ( $234 \text{ K} < T < 244 \text{ K}$ ), the QENS spectra for the wet sample can be fit with a single Lorentzian that yields a diffusion coefficient  $D$  showing an upward substep on heating, which appears neither for the *dry* sample nor for the *wet* sample on cooling. The upward substep in  $D$  near 237 K suggests

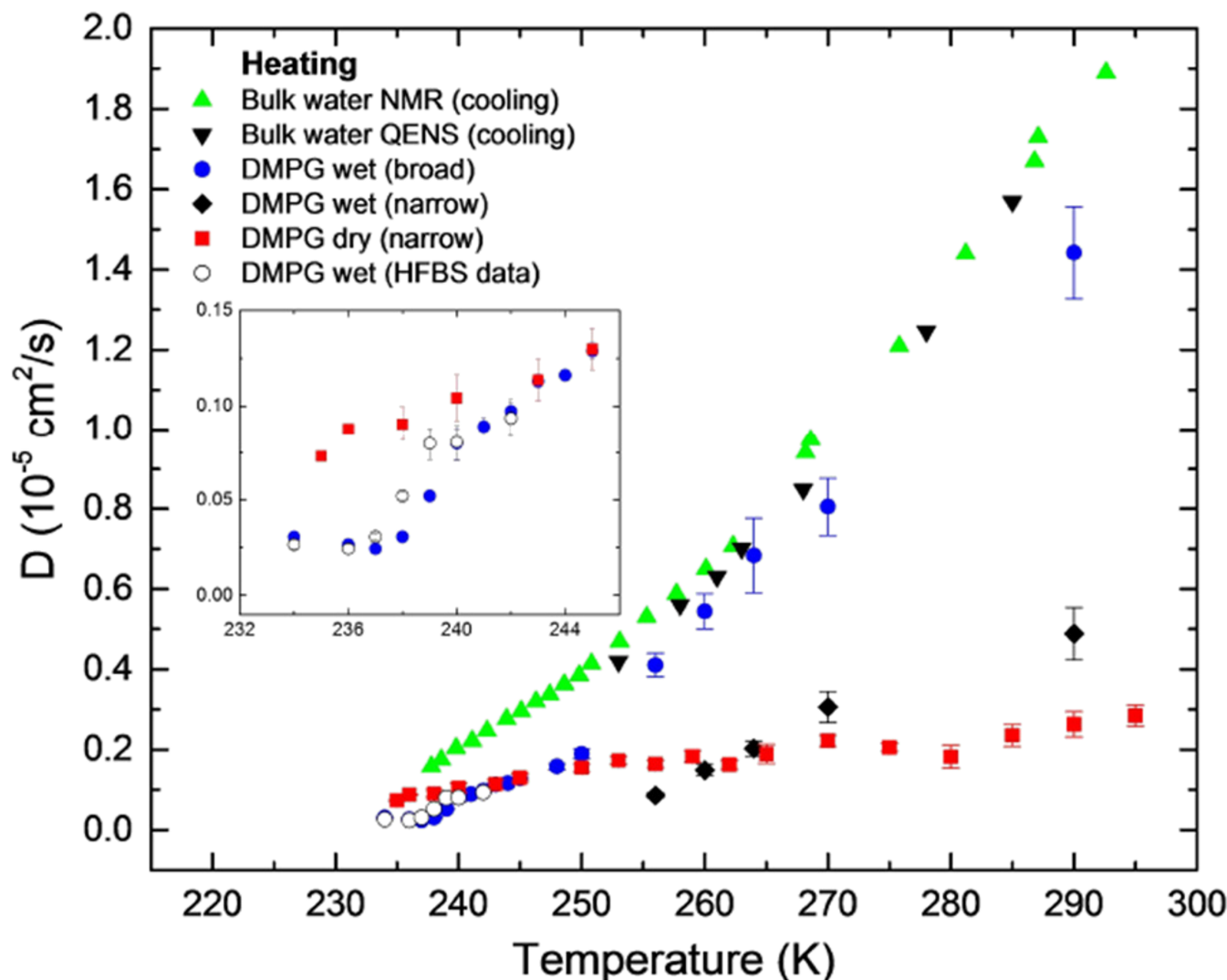


FIG. 9. Diffusion coefficients  $D$  inferred from the analysis of the QENS spectra of both wet and dry DMPG samples as a function of temperature on *heating*. Data points are coded as in Fig. 8. Inset shows low temperature data on an expanded scale. Open black circles indicate data taken on the HFBS at NIST. All other diffusion coefficients were determined from spectra collected on BASIS.

a melting transition of some component of water as will be discussed Sec. IV A. At higher temperatures ( $T > 240$  K), the diffusion coefficients of the wet and dry samples are similar to those obtained on cooling. In particular, both the wet and dry samples show evidence of a water component undergoing weakly temperature-dependent translational diffusion at a rate well below that of bulk supercooled water.

#### 4. Search for bound water

In our study of both wet and dry DMPC membranes,<sup>8</sup> we found evidence of a weak narrow-Lorentzian component in their QENS spectra with a FWHM  $\sim 5$   $\mu\text{eV}$  that was nearly  $Q$ -independent. We attributed the intensity of this narrow component to scattering from the H atoms in the lipid molecules plus H atoms in water molecules bound to the lipid head groups that all moved on the same nanosecond time scale. We now turn to the question of whether there is also evidence of such bound water molecules in the spectra of the DMPG membranes.

The search for a bound-water component in the QENS spectra is more difficult in the case of the wet DMPG sample

because of the presence of the narrow-Lorentzian component (FWHM  $\sim 30$   $\mu\text{eV}$ ) whose intensity is up to half that of the broad-Lorentzian component for  $T > 260$  K [see Figs. 6(b) and 6(c)]. These two components would tend to mask a third Lorentzian component that is comparable in magnitude to the narrow-Lorentzian component and having a FWHM  $\sim 5$   $\mu\text{eV}$  as was the case for the bound water in the DMPC membrane. For these reasons, the bound water component should be easiest to observe at high temperature and high  $Q$  where the broad Lorentzian merges with the background scattering. We have found some evidence for a weak third Lorentzian in the QENS spectra of the dry DMPG sample at temperatures in the range 275 K to 290 K; however, it is difficult to quantify its intensity and FWHM.

## IV. DISCUSSION

The analysis of the QENS spectra of our DMPG samples provides support for the different types of membrane-associated water that we have inferred from the temperature dependence of the elastically scattered-neutron intensity.<sup>9</sup>

## A. Water above the membrane

As shown in Fig. 8, on cooling in the temperature range  $253\text{ K} < T < 270\text{ K}$ , the diffusion coefficients inferred from the broad-Lorentzian component in the spectra of the wet DMPG sample are in reasonable agreement with those of bulk supercooled water determined by both QENS and NMR measurements. Therefore, we have identified the broad-Lorentzian component in the spectra of the wet sample with “bulk-like” water located above the membrane, which is in excess of that needed to fully hydrate it.

To estimate the fraction of the total amount of water in the wet sample that is bulk-like, we assume that the increment in the elastic intensity as the sample is cooled from 262 K to 253 K [indicated by the length of the vertical double-arrow labeled “1c” in Fig. 2(b)] is proportional to the amount of bulk-like water that freezes. It is about 50% of the total increase in the elastic intensity from the highest to the lowest temperatures, which we have seen corresponds to an effective water slab thickness of  $\sim 71\text{ nm}$  (see Sec. II A). Therefore, we estimate the effective thickness of the bulk-like water to be  $\sim 35\text{ nm}$  for the wet DMPG sample. The amount of bulk-like water scales roughly with a sample’s total water content. As can be seen in Fig. 4, the increment in the elastic intensity on cooling in temperature Region 1 decreases nearly in proportion to the sample’s effective water thickness for samples (a)–(c).

It is interesting to note that even as the bulk-like water is freezing in the temperature range  $253\text{ K} < T < 262\text{ K}$ , the value of the diffusion coefficient  $D$  remains close to that of bulk water as shown in Fig. 8. That is,  $D$  provides no evidence of confined water in this temperature range. However,  $D$  begins to decrease more rapidly than for bulk water just below 253 K, i.e., on entering temperature Region 2 of Fig. 4 ( $230\text{ K} < T < 251\text{ K}$ ) where the elastic intensity increases linearly with decreasing temperature. This behavior suggested us that water in a different local environment could be freezing. We refer to this water as “confined 1” to distinguish it from “confined 2” water that we associate with the narrow-Lorentzian component in the spectra of the wet DMPG sample as will be discussed below. To estimate the amount of confined 1 water, we use the increment in the elastic intensity that occurs in Region 2 on cooling. Although they are shifted upward in temperature due to hysteresis, the boundaries of Region 2 can be seen more clearly in the heating curve in Fig. 2(b) as a substep at  $\sim 240\text{ K}$  and a weaker one at  $\sim 260\text{ K}$ . Between these substeps is an intensity decrement labeled “2h” equal in magnitude to the increment “2c” observed on cooling. Proceeding as we did above for the bulk-like water, we assume that the length of the vertical double-arrow labeled “2c” in Fig. 2(b) is proportional to the amount of confined 1 water that freezes in Region 2. In this way, we estimate the effective thickness of the confined 1 water to be  $\sim 24\text{ nm}$ . Although the relatively large amount of bulk-like and confined 1 water in the wet sample implies that they are both located above the membrane, the confined 1 water, which freezes at lower temperatures, is presumably closer to the lipid head groups. Confined 1 water also differs from bulk-like water in that its amount does not scale with the total water content of a sample. We see in Fig. 4 that the slope of the linear intensity increase in temperature Region 2

is nearly the same for the three samples with the highest water content, indicating that about the same amount of confined 1 water is freezing.

To substantiate the presence of confined 1 water, we have also examined the temperature dependence of the diffusion coefficient  $D$  inferred from the analysis of the QENS spectra of the wet DMPG sample. As described above, we were able to fit the spectra in the temperature range  $253\text{ K} < T < 270\text{ K}$  with two Lorentzians. However, attempts at a two-Lorentzian fit in the range  $240\text{ K} < T < 251\text{ K}$  gave a poorer fit to the spectra than a single Lorentzian. We interpret the failure of a two-Lorentzian fit as indicating that the difference in the diffusion rate of “fast” and “slow” water is too small to resolve so that only an average  $D$  can be determined. The steep drop in this average  $D$  below that of bulk supercooled water for  $T < 251\text{ K}$  (see Fig. 8) correlates with the freezing of confined 1 water that we have inferred from the elastic intensity scans. We conclude that there is a component of the membrane-associated water termed confined 1, which is presumably located in the space between the frozen bulk-like water and the membrane [see Fig. 1(a)] and whose confinement imposes a reduction of its average diffusion coefficient relative to supercooled bulk water. However, with an effective thickness of  $\sim 24\text{ nm}$ , confined 1 water would presumably be indistinguishable from bulk-like water above a temperature of 269 K at which the melting of bulk-like ice is complete.

On cooling below 240 K, all of the confined 1 water freezes out, leaving water termed confined 2 having a diffusion coefficient smaller than that of confined 1 water and matching the value inferred from the narrow-Lorentzian component of the dry sample (see Fig. 8). The smaller diffusion coefficient of confined 2 water suggests that it is located around the head groups of the lipids and inside the membrane (see below).

As discussed in Ref. 9, a single-supported wet DMPC membrane also shows evidence of both bulk-like and two types of confined water. Despite differences between our DMPC and DMPG samples in the freezing/melting behavior of their membrane-associated water as revealed by the elastic intensity scans in Fig. 2, the temperature dependence of their water diffusion coefficients show common features as can be seen in Fig. 8. Above 270 K, the value of  $D$  inferred for the DMPC sample is close to that of the DMPG sample, both of which track the diffusion coefficient for bulk supercooled water obtained from QENS<sup>26</sup> and NMR<sup>27</sup> measurements. On cooling from 270 K to 265 K, the diffusion coefficient of the water in the DMPC sample decreases more steeply before leveling off. We interpret this temperature dependence of  $D$  as indicating the freezing of bulk-like water, which leaves still mobile confined 1 water. Then, a second steep decrease in  $D$  occurs on cooling the DMPC sample from 263 K to 260 K, which, in analogy to the behavior of the DMPG sample, we attribute to the freezing out of confined 1 water, leaving still mobile confined 2 water. As discussed in Ref. 9, this transition is more difficult to identify in the elastic intensity of the DMPC sample [see Fig. 2(a)]. In contrast to DMPG, it has proved impossible to isolate a contribution of confined 2 water in coexistence with bulk-like water in the QENS spectra of the DMPC membrane at higher temperatures.

While the DMPC and DMPG samples both show evidence of bulk-like and confined 1 water in the freezing behavior, there are qualitative differences in their melting behavior that suggest an additional water type may be present above the DMPG membrane. On heating, the DMPC sample shows only one large and relatively abrupt downward step near the bulk melting point of 273 K [Fig. 2(a)]. In contrast, the two DMPG samples with the greatest water content show a succession of three downward substeps in their elastic intensity on heating [labeled 3h, 2h, and 1h in Fig. 2(b)]. Because the intensity decrement in each one of these substeps is equal in magnitude to the corresponding intensity increments observed on cooling labeled 3c, 2c, and 1c that we have identified with freezing transitions, we interpret these intensity substeps on heating as indicating successive melting transitions. Specifically, the 1h and 2h substeps would correspond to the melting of bulk-like and confined 1 water, respectively. However, a question remains as to the origin of the 3h substep. The increase in the water diffusion coefficient by almost a factor of 5 on heating through the 3h substep (see circles in the inset of Fig. 9) is consistent with a melting transition. Performing a similar analysis of the decrement in the elastic intensity at the 3h-substep on heating as we used for the 1c and 2c intensity increments on cooling, we estimate the effective thickness of the water that is melting to be  $\sim 13$  nm. Again, this amount of water is too large to be confined within the membrane. The hysteresis indicated by the narrow width of the 3h substep on heating compared to the temperature range over which the 3c intensity increment occurs on cooling [see Fig. 2(b)] perhaps suggests water confined to a narrow pore in ice. The absence of such a melting transition in the wet DMPC sample may indicate that its ice has a different morphology. Neutron diffraction measurements in progress on both DMPG and DMPC samples may elucidate the structure of the solid, membrane-associated water.<sup>28</sup>

## B. Water within the membrane

We next consider the narrow-Lorentzian component identified in the spectra of the wet DMPG sample. In Fig. 8, we have seen that, on cooling in the temperature range  $253 \text{ K} < T < 263 \text{ K}$ , the diffusion coefficients inferred from the narrow-Lorentzian component for the wet DMPG sample agree well with those obtained from fits to spectra of the dry DMPG sample over a much wider temperature range. This agreement in the water dynamics of the wet and dry samples, whose water content differ by a factor of three, supports identifying the narrow-Lorentzian component with a similar type of water present in both samples, which we have denoted as “confined 2.” Furthermore, the comparable *intensity* of the narrow-Lorentzian component in the wet and dry samples [see Fig. 6(c)] indicates that there is about the same amount of confined 2 water in the two samples. These features suggest that confined 2 water is bound more strongly and located closer to the lipid head groups than the confined 1 and bulk-like water.

As pointed out in Sec. III B 2, the diffusion coefficient of the confined 2 water has a weaker temperature dependence than the bulk-like and confined 1 water (see Figs. 8 and 9). We find a gradual change in the water diffusion coefficient over a wide temperature range,  $220 \text{ K} < T < 295 \text{ K}$ ,

without evidence of a well-defined freezing/melting transition. At 295 K, the confined 2 water has a value of  $D = 3.0 \times 10^{-6} \text{ cm}^2/\text{s}$ , which is about a factor of 7 smaller than for bulk water; and it decreases on cooling to a value of  $0.2 \times 10^{-6} \text{ cm}^2/\text{s}$  at 230 K, which is comparable to that of bulk supercooled water. We speculate that the confined 2 water could be exhibiting a continuous freezing/melting behavior between a fluid and a solid amorphous phase.

Due to the small quantity of confined 2 water, it is most easily studied in the dry DMPG sample (effective water thickness  $\sim 23$  nm). However, its gradual freezing/melting behavior makes it difficult to estimate the amount of confined 2 water from changes in the elastic intensity on cooling and heating [see Fig. 3(d)] as we have done for the bulk-like and confined 1 water in the wet sample. Therefore, we have used another method to infer its effective thickness that has been applied to our analysis of simulated spectra of freestanding DMPG membranes.<sup>14</sup> At temperatures  $T > 280 \text{ K}$ , all the water in the dry sample is fluid and moving on a time scale such that it does not contribute elastic scattering to the BASIS spectra. We then estimate the fraction of confined 2 water from the ratio of the narrow-Lorentzian intensity to that of the total quasielastic intensity, the sum of the narrow- and broad-Lorentzian intensities. To check that the intensity of the elastic scattering is in fact negligible, we calculate the fraction of confined 2 water so defined as a function of  $Q$ . Because we expect the elastic scattering to decrease as  $Q$  increases, we assume that the elastic component has vanished when  $Q$  reaches a value where the fraction of confined 2 water has become  $Q$ -independent.<sup>14</sup> In this way, we estimate an effective thickness of  $\sim 2.3$  nm for the confined 2 water. Assuming it to have the density of bulk water, this thickness is equivalent to  $\sim 18 \pm 8$  water molecules per lipid. This value is greater than  $\sim 10$  water molecules/lipid estimated to be required for the full hydration of the membrane from MD simulations.<sup>14</sup> We also point out that the estimated effective thickness of the confined 2 water is comparable to that of the water layer between the lower leaflet of a DMPC membrane and the  $\text{SiO}_2$  surface [see Fig. 1(a)], i.e., a thickness of  $\sim 1$  nm as determined by neutron reflectivity measurements<sup>21</sup> and by interferometry.<sup>29</sup> Therefore, we cannot exclude the possibility that the water between the membrane and the substrate is also contributing to the confined 2 water signal, which would have the effect of reducing our estimate of the number of water molecules per lipid.

## C. Applicability of a jump diffusion model

There is evidence in Fig. 7 of a leveling off of the FWHM at high  $Q$  for both the broad- and narrow-Lorentzian components as predicted in models of jump diffusion.<sup>26</sup> To investigate how well a jump diffusion model describes the dynamics of the membrane-associated water in our DMPG samples, we fit the half-width of the Lorentzian components representing the quasielastic scattering,  $\Gamma(Q) = \text{FWHM}/2\hbar$ , to Eq. (4) in Ref. 26,

$$\Gamma(Q) = \frac{DQ^2}{1 + DQ^2\tau_0}, \quad (1)$$

where  $\tau_0$  is the residence time. For temperatures  $T > 250 \text{ K}$ , we found that the values of the diffusion coefficient  $D$  obtained by

fitting Eq. (1) to the broad-Lorentzian component of the wet DMPG sample and the narrow component of the dry sample were systematically higher and had larger error bars than those determined by assuming a linear dependence of the FWHM on  $Q^2$  (Fick's law) at low  $Q$  as plotted in Fig. 8. More importantly, the  $D$  values obtained by fitting to Eq. (1) were also larger than those obtained for bulk supercooled water by QENS<sup>26</sup> and NMR.<sup>27</sup> Therefore, we limited our analysis of the residence times to temperatures  $T < 250$  K where we obtained reasonable agreement of the diffusion coefficients  $D$  of both DMPG samples with those shown in Fig. 8.  $\tau_0$  inferred from the broad-Lorentzian component in the spectra of the wet sample agrees well with that found for bulk water<sup>26</sup> at a temperature of 253 K and then rises as the temperature is lowered (see Fig. S2 in the [supplementary material](#)).

The analysis of the narrow-Lorentzian component in the dry sample representing confined 2 water nearest the lipid head groups yielded residence times with little temperature dependence within the measurement uncertainty (compared to  $D$ , which decreases by a factor of 5 as the temperature is reduced from 250 K to 229 K). This behavior reflects the weak temperature dependence and large error bars for the FWHM of the narrow-Lorentzian component in the spectra of the dry sample at high  $Q$ . For  $T < 250$  K, we estimate residence times  $\tau_0$  in the range 50–90 ps, which contains the values to which the wet sample rises near 235 K as shown in Fig. S2 of the [supplementary material](#). Thus, at low temperatures, not only does the water dynamics of the wet sample approach that of the dry sample on a large length scale as indicated by their comparable diffusion coefficients (see Fig. 8) but also on a shorter length scale as indicated by their comparable residence times. Because of the relatively weak QENS spectra of our DMPG membrane samples compared to those of bulk water,<sup>26</sup> we did not pursue an analysis of the jump diffusion model further.

#### D. Comparison with molecular dynamics simulations

Our MD simulations<sup>14</sup> have investigated the structure and dynamics of water and lipid molecules in a freestanding DMPG bilayer similar to simulations reported earlier on a DMPC membrane.<sup>10</sup> The DMPG simulations were conducted at a temperature of 310 K, which is the same reduced temperature (relative to the gel-to-fluid transition temperature) as used in the DMPC simulations. In this section, we compare the diffusion coefficients that have been inferred from the simulation as a function of depth in the membrane with those of bulk-like water and confined 2 water inferred from our measurements. Unfortunately, the simulations could not be done easily at the lower temperatures of the experiments due to the very long equilibration times. Also, the experiments were difficult to conduct at higher temperatures due to the limited dynamic range of the HFBS and BASIS spectrometers ( $< 120$   $\mu$ eV). Therefore, to compare simulations with the experiment requires the extrapolation of the diffusion coefficients inferred from measurements at temperatures  $T \leq 295$  K to 310 K, the temperature of the simulation. We emphasize that one must be cautious in comparing our measurements on single-supported membranes with results of MD simulations on freestanding membranes. As yet, the detailed mechanism binding a bilayer via a water layer to an SiO<sub>2</sub> surface

is uncertain; and the effect of the substrate on the membrane structure and dynamics has not been quantified. We are currently conducting simulations of a well-hydrated DMPC bilayer supported on an SiO<sub>2</sub> surface.

Before making this comparison, we recall that a key result of the simulations was the effect of the counter ion valency in determining the phase of the DMPG membrane.<sup>14</sup> At 310 K, the freestanding membrane is in the fluid phase with a monovalent counter ion (Na<sup>+</sup>), whereas it is in the gel phase with a divalent counter ion (Ca<sup>++</sup>). The simulations suggest that the gel phase is stabilized by the high affinity of the divalent cation to the phosphate group, allowing it to bind simultaneously to two different lipid molecules. Because the single-supported membranes investigated experimentally are believed to be in the gel phase,<sup>8,19</sup> we restrict comparison to the simulation results with the divalent counter ion.

From Fig. 8, we see that the observed QENS spectra of the wet DMPG sample at 295 K yield a diffusion coefficient  $D = 1.7 \times 10^{-5}$  cm<sup>2</sup>/s. Assuming the same temperature dependence of  $D$  as found in the NMR measurements on bulk water<sup>27</sup> (green up triangles in Fig. 8) and extrapolating to the simulation temperature of 310 K, we estimate  $D = 2.3 \times 10^{-5}$  cm<sup>2</sup>/s compared to the value of  $D = 2.5 \times 10^{-5}$  cm<sup>2</sup>/s inferred from the analysis of the broad-Lorentzian component in the simulated spectra.<sup>14</sup> We believe that the difference in these values is within the uncertainty imposed by the limited dynamic range of BASIS and the error in extrapolation. In the analysis of both the experiment and the simulation, we have identified the broad-Lorentzian component with bulk-like water located above the membrane. Because the QENS measurements were done on samples having a higher water content than in the simulations, we would expect them to yield a  $D$  closer to the bulk value. In fact, in the temperature range 253 K  $< T < 270$  K, where the width of the quasielastic scattering is within the dynamic range of BASIS, the values of  $D$  inferred for the wet DMPG are in good agreement with those inferred for bulk supercooled water by QENS<sup>26</sup> and NMR.<sup>27</sup>

The MD simulations also allow a determination of the diffusion coefficients of the hydration water as a function of the depth in the membrane. Table I of Ref. 14 gives the values of  $D$  computed from the mean-square displacement of the water molecules in slabs 7.5 Å thick as one moves outward along the membrane normal, beginning at the phosphorous atom position in the DMPG head group. We can compare these values of  $D$  with those obtained for confined 2 water from the analysis of the narrow-Lorentzian component in the QENS spectra of the dry DMPG sample, which presumably represents the dynamics of water closest to the lipid head groups. We have seen that the values of  $D$  inferred from the narrow-Lorentzian component yield a temperature dependence 6 times weaker than that of the bulk-like water above the membrane, which facilitates extrapolation. Linearly extrapolating the  $D$  values determined on heating the dry DMPG sample in the temperature range 273  $< T < 295$  K (see Fig. 9), we estimate  $D \sim 4 \times 10^{-6}$  cm<sup>2</sup>/s at 310 K, the temperature of the simulation. This value is reasonably close to  $5.0 \times 10^{-6}$  cm<sup>2</sup>/s found in the simulation for the slab which has its inner boundary at the position of the phosphorous atom in the DMPG head group.

The narrow-Lorentzian component in the fit to the *simulated* QENS spectra of the DMPG membrane in the gel phase is more difficult to reconcile with our experimental results. First, its intensity is very weak, corresponding to only  $\sim 2.1$  water molecules per lipid, which is probably too small to be resolved in the observed spectra. Second, the width of the narrow-Lorentzian component in the simulated spectra does not show a  $Q^2$  dependence at low  $Q$  characteristic of translational diffusion (see Fig. 7). For this reason, the narrow-Lorentzian component in the simulations has been tentatively identified with water molecules bound to the lipid head group.<sup>14</sup> We speculate that, at the higher temperature of the simulation, the slow translational diffusion in the head group region and motion of bound water are too close in time scale to be resolved.

## V. SUMMARY AND CONCLUSION

Here we summarize the different water types that we have identified in our samples of single-supported zwitterionic and anionic membranes. We first describe water types common to both membranes, then point out some differing features, and finally discuss some open questions.

### A. Common features of water types associated with zwitterionic and anionic membranes

We have found our samples of single-supported zwitterionic (DMPC) and anionic (DMPG) bilayer membranes to be simple and homogeneous enough to allow different types of water that are common to both membranes to be distinguished. These water types are presumably determined by their local environment, which is characterized by the proximity of the water molecules to the lipid head groups, the strength of the water-head group interactions and, at low temperatures, by the proximity of water molecules to bulk ice. In addition to mobile “bulk-like” water furthest from the lipid head groups, we have identified water types termed “confined 1” and “confined 2,” as depicted in Fig. 1(a), in closer proximity to the membrane. Because we find evidence of confined 1 water only below the freezing point of bulk-like water and in a relatively large amount (effective thickness  $\sim 23$  nm), we have suggested that it is confined to the region between bulk ice and the lipid head groups. Above the melting point of bulk ice, bulk-like and confined 1 water are believed to move on the same time scale and therefore would be indistinguishable in a QENS experiment. Based on the analysis of the DMPG QENS spectra, we posit that the slower-moving confined 2 water (effective thickness  $\sim 2.3$  nm) is localized within and just outside the lipid head group region.

In the case of the dry DMPG membrane,  $D$  of the confined 2 water can be tracked over a wide temperature range from 295 K down to 220 K. This behavior is consistent with continuous freezing of the confined 2 water over this wide temperature range. We speculate that it forms an amorphous solid at the lowest temperature. Extrapolating the diffusion coefficient  $D$  of the confined 2 water to a temperature of 310 K at which an MD simulation of a freestanding DMPG membrane in its gel phase has been performed<sup>14</sup> yields a value of  $D$  within the range found in the simulation for water in the head-group region.

For both the wet and dry DMPC membranes, we identify confined 2 water as that which remains mobile below the freezing of bulk-like and confined 1 water. In Fig. 8, we see that  $D$  decreases to a nearly constant value in a narrow temperature range below 260 K. It is noteworthy that at 260 K the confined 2 water in DMPC has  $D \sim 4 \times 10^{-6}$  cm<sup>2</sup>/s, which is about 4 times greater than that of confined 2 water in the DMPG sample. Unlike DMPG, we are unable to observe confined 2 water in coexistence with bulk-like water at higher temperatures in the QENS spectra of the DMPC samples. Also, it is difficult to quantify the amount of confined 2 water from the temperature dependence of the elastic intensity of the DMPC samples.

As already noted, both the DMPG and DMPC membranes only show evidence of confined 1 water on cooling to temperatures below the freezing of bulk-like water. Therefore, we have suggested that the freezing behavior of confined 1 water may be determined by its proximity to overlying bulk ice as well as the lipid head groups beneath it. For the wet DMPG sample, this freezing behavior is characterized on cooling by the nearly linear increase of the elastic neutron intensity in temperature Region 2 of Fig. 4 and the steep decrease in  $D$  in this temperature range (Fig. 8). The dry DMPG sample appears to have less confined 1 as well as bulk-like water so that we have been unable to determine a value of  $D$  for either.

For the wet and dry DMPC samples, we identify confined 1 water from the temperature dependence of the elastic neutron intensity as the dominant contributor to the region of continuous freezing just below the step-like freezing transition of the bulk-like water [see Fig. 2(a)]. This identification is supported by the steep decrease in  $D$  near 262 K for both the wet and dry DMPC samples (see Fig. 8).

The melting behavior of the membrane-associated water in the DMPG and DMPC samples also provides evidence of confined 1 water. In the wet DMPG sample, the melting of the confined 1 water is characterized by the substep in the elastic neutron intensity labeled 2h in Fig. 2(b), which is followed by the melting of bulk-like water represented by a substep labeled 1h. Consistent with its smaller amount of confined 1 water, the dry DMPG sample does not have a substep in its elastic intensity on heating corresponding to the 2h substep of the wet DMPG sample [cf. Figs. 2(b) and 3(d)].

In contrast, the wet DMPC sample on heating shows a large step-like decrease in the elastic intensity [see Fig. 2(a)] at the bulk melting point. The downturn in the elastic intensity beginning  $\sim 5$  K above the step may correspond to the melting of confined 1 water.

In the case of the DMPC membrane, we could identify a contribution to the quasielastic spectra from water that moved on the same time scale ( $\sim 1$  ns) as the H atoms in the lipid molecules.<sup>8</sup> For the DMPG membrane, we have found some evidence of such bound water represented by a narrow component in the quasielastic spectra near room temperature but have been unable to quantify its amount. The MD simulations<sup>14</sup> indicate only a small component of bound water ( $\sim 2$  water molecules per lipid), which would render it difficult to observe in our experiment. Thus, in the case of the wet DMPG membrane, the QENS spectra provide evidence of bulk-like water, confined 1 and confined 2 water, and possibly bound water.

## B. Differing features of the water associated with zwitterionic and anionic membranes

Even though the QENS spectra represent an average over all of the membrane-associated water, the diffusive motion of water in the head group region of both membranes is sufficiently slower than that of bulk-like and confined 1 water that it has been possible to extract its contribution to the spectra. We find a difference between the zwitterionic and anionic membranes in the type of diffusive motion of water in the head group region that is observable in their QENS spectra. For the zwitterionic membrane (DMPC) above a temperature of 270 K, the dominant contribution to the observed QENS spectra by water in the head group region is from molecules that move on the same time scale as H atoms in the lipid, i.e., water molecules that we have referred to as “bound.”<sup>8</sup> This diffusive motion is nearly  $Q$ -independent.<sup>8,19</sup> In the case of the anionic DMPG membrane above 270 K, the water in the head group region that contributes dominantly to the QENS spectra consists of confined 2 water, i.e., molecules undergoing translational diffusion (FWHM  $\sim Q^2$  at low  $Q$ ) at a rate faster than “bound” water but more slowly than the bulk-like and confined 1 water. We attribute this difference in water dynamics to the larger number of bound water molecules in DMPC than for DMPG. From our QENS measurements on DMPC (Ref. 8) in the gel phase, we estimated 7–10 water molecules bound per lipid, while  $\sim 4$  per lipid has been determined by NMR (Ref. 30). These values are larger than the  $\sim 2$  water molecules bound per lipid for DMPG in its gel-phase as inferred from our MD simulations (Ref. 14).

Another indication of a difference in the water/head group interaction between the zwitterionic and anionic membranes is the freezing/melting behavior of the interfacial water in the wet samples. From the temperature scans of the elastic neutron intensity in Fig. 2, we see that the wet anionic membrane (DMPG) has a much greater width to its freezing/melting transitions than the zwitterionic membrane (DMPC). Also, in the melting of the DMPG sample, there appears to be an extra substep labeled 3h [Fig. 2(b)] in the elastic intensity, which is absent for the DMPC sample. In addition, the substep labeled 2h that we have identified with the melting of confined 1 water in the wet DMPG sample cannot be resolved for DMPC.

Besides a different water/head group interaction in the zwitterionic and anionic membranes, we have also considered two other sources of the disparity in their elastic scans and QENS spectra: (1) a difference in their monovalent and divalent salt concentration; and (2) a difference in membrane/substrate interaction. With regard to salt effects, we note a variation in our preparation of the two membranes. In the case of DMPC, the salt solution used in the deposition process was rinsed away along with bilayer fragments above the complete membrane adjacent to the SiO<sub>2</sub> surface. However, for the DMPG sample, the membrane was too fragile to withstand rinsing so that its final salt content may have been higher. The reduction in the onset temperature of freezing as the water content of the DMPG samples decreases (see Fig. 3) might be explained by a corresponding increase in salt concentration. We note, though, that fusion of uniformly thick and homogeneous DMPG bilayers to the SiO<sub>2</sub>

surface only occurs in a narrow concentration range of the divalent salt,  $\sim 15$  mM (see Ref. 19), which may tend to maintain the divalent salt concentration between samples. Also, the reproducibility of the DMPG elastic scans and QENS spectra for a given water content suggests that either the salt content is constant between these samples or that our QENS results are insensitive to salt concentrations at the levels present.

We view the principal effect of the phospholipids' interaction with the substrate to be the stabilization of the gel phase for both membranes. It seems likely that the presence of the substrate could affect the dynamics of the water in the layer between the proximal leaflet and the SiO<sub>2</sub> surface, but we would expect a smaller effect for water surrounding the distal leaflet. MD simulations will be helpful in investigating these effects.

Thus, the combination of the water/head group interaction, the salt content, and the membrane/substrate interaction may cause the different freezing/melting behavior and water dynamics observed for the two membranes. Although we cannot yet separate these factors experimentally, it may be possible to isolate their effect in MD simulations. This combination of factors may also manifest itself in how ice wets the membranes. For example, the more hydrophilic DMPG membrane might wet a solid amorphous film of uniform thickness rather than support a powder of ice crystals. Neutron diffraction experiments now in progress<sup>28</sup> should help elucidate the structure of frozen water in proximity to both the DMPC and DMPG membranes.

## C. Open questions

Our results raise a number of questions related to the freezing/melting behavior and the dynamics of the interfacial water associated with these model zwitterionic and anionic membranes. For both DMPG and DMPC, how can the freezing behavior and dynamics of the confined 1 water apparently located so far from the membrane ( $\sim 20$ – $30$  nm) be affected by the charge and structure of the lipid head group? Are these properties of confined 1 water influenced by the presence of frozen bulk water above it and the salt concentration? Why is the freezing of water associated with the DMPG membrane spread out over such a wide temperature range below the bulk water triple point at 273 K? What is the origin of the melting transition represented by the 3h substep in the elastic neutron intensity of the wet DMPG samples and why is it absent in the dry sample?

In conclusion, single-supported bilayers of the zwitterionic DMPC and anionic DMPG membranes provide useful model systems for comparing the structure and dynamics of their membrane-associated water. We have found the freezing/melting behavior and the translational diffusive motion of the membrane-associated water on nano-length and time scales to be sensitive to the structure and charge of the lipid head group. Despite differences in their structure and dynamics, the interfacial water in the zwitterionic and anionic membranes appear to share a classification scheme of water types based on the proximity of the water to the membrane: bulk-like, confined 1, confined 2, and bound water. Of these, confined 1 water has been identified only

in coexistence with bulk ice and hence is not present at biologically relevant temperatures. It is expected that further study combining both QENS and MD simulations will reveal greater details of the water/lipid head group interaction and eventually the interaction of water with integral membrane proteins.

## SUPPLEMENTARY MATERIAL

See [supplementary material](#) for Atomic Force Microscopy (AFM) images of single-supported DMPC and DMPG membranes (Fig. S1) and the temperature dependence of the residence time in a jump diffusion model for the wet and dry DMPG samples (Fig. S2).

## ACKNOWLEDGMENTS

This work was supported by the U.S. National Science Foundation under Grant Nos. DMR-0705974 and DGE-1069091 and utilized facilities supported in part by the National Science Foundation under Agreement No. DMR-1508249. Facilities supported by the Danish Center for High Performance Computing are also acknowledged. A portion of this research at Oak Ridge National Laboratory's Spallation Neutron Source was sponsored by the Scientific User Facilities Division, Office of Basic Energy Sciences, U.S. Department of Energy. We thank Dan A. Neumann, Matthew McCune, and Ioan Kosztin for helpful discussions.

<sup>1</sup>S. König, E. Sackmann, D. Richter, R. Zorn, C. Carlile, and T. M. Bayerl, *J. Chem. Phys.* **100**, 3307 (1994).

<sup>2</sup>W. Pfeiffer, Th. Henkel, E. Sackmann, W. Knoll, and D. Richter, *Europhys. Lett.* **8**, 201 (1989).

<sup>3</sup>S. König, W. Pfeiffer, T. Bayerl, D. Richter, and E. Sackmann, *J. Phys. II* **2**, 1589 (1992).

<sup>4</sup>M. C. Rheinstädter, T. Seydel, F. Demmel, and T. Salditt, *Phys. Rev. E* **71**, 061908 (2005).

<sup>5</sup>J. Swenson, F. Kargi, P. Bernsten, and C. Svanberg, *J. Chem. Phys.* **129**, 045101 (2008).

<sup>6</sup>M. Trapp, T. Gutberlet, F. Juranyi, T. Unruh, B. Demé, M. Tehei, and J. Peters, *J. Chem. Phys.* **133**, 164505 (2010).

<sup>7</sup>L. Topozini, F. Roosen-Runge, R. I. Bewley, R. M. Dalgliesh, T. Perring, T. Seydel, H. R. Glyde, V. García Sakai, and M. C. Rheinstädter, *Soft Matter* **11**, 8354 (2015).

<sup>8</sup>M. Bai, A. Miskowiec, F. Y. Hansen, H. Taub, T. Jenkins, M. Tyagi, S. O. Diallo, E. Mamontov, K. W. Herwig, and S.-K. Wang, *Europhys. Lett.* **98**, 48006 (2012).

<sup>9</sup>A. Miskowiec, Z. N. Buck, M. C. Brown, H. Kaiser, F. Y. Hansen, G. M. King, H. Taub, R. Jiji, J. W. Cooley, M. Tyagi, S. O. Diallo, E. Mamontov, and K. W. Herwig, *Europhys. Lett.* **107**, 28008 (2014).

<sup>10</sup>F. Y. Hansen, G. H. Peters, H. Taub, and A. Miskowiec, *J. Chem. Phys.* **137**, 204910 (2012).

<sup>11</sup>J. Das, E. Flenner, and I. Kosztin, *J. Chem. Phys.* **139**, 065102 (2013).

<sup>12</sup>Y. von Hansen, S. Gekle, and R. R. Netz, *Phys. Rev. Lett.* **111**, 118103 (2013).

<sup>13</sup>J. Yang, C. Calero, and J. Martí, *J. Chem. Phys.* **140**, 104901 (2014).

<sup>14</sup>A. K. Rønneest, G. H. Peters, F. Y. Hansen, H. Taub, and A. Miskowiec, *J. Chem. Phys.* **144**, 144904 (2016).

<sup>15</sup>E. T. Castellana and P. S. Cremer, *Surf. Sci. Rep.* **61**, 429 (2006).

<sup>16</sup>S.-K. Wang, E. Mamontov, M. Bai, F. Y. Hansen, H. Taub, J. R. D. Copley, V. García Sakai, G. Gasparovic, T. Jenkins, M. Tyagi, K. W. Herwig, D. Neumann, W. Montfrooij, and U. G. Volkman, *Europhys. Lett.* **91**, 66007 (2010).

<sup>17</sup>Certain commercial equipment, instruments, or materials (or suppliers) are identified in this paper to foster understanding. Such identification does not imply recommendation or endorsement by the National Institute of Standards and Technology, nor does it imply that the materials or equipment identified are necessarily the best available for this purpose.

<sup>18</sup>L. Picas, C. Suárez-Germà, M. T. Montero, and J. Hernández-Borrell, *J. Phys. Chem. B* **114**, 3543 (2010).

<sup>19</sup>A. Miskowiec, Ph.D. thesis, University of Missouri, 2014.

<sup>20</sup>A. Miskowiec, Z. N. Buck, P. Schnase, H. Kaiser, T. Heitmann, P. F. Miceli, M. Bai, H. Taub, F. Y. Hansen, G. M. King, M. Dubey, S. Singh, and J. Majewski, "Temperature dependence of the thickness of DMPC and DMPG membranes measured by Atomic Force Microscopy" (unpublished).

<sup>21</sup>S. J. Johnson, T. M. Bayerl, D. C. McDermott, G. W. Adam, A. R. Rennie, R. K. Thomas, and E. Sackmann, *Biophys. J.* **59**, 289 (1991).

<sup>22</sup>J. F. Nagle, R. Zhang, S. Tristram-Nagle, H. I. Petrache, and R. M. Suter, *Biophys. J.* **70**, 1419 (1996).

<sup>23</sup>E. Mamontov and K. W. Herwig, *Rev. Sci. Instrum.* **82**, 085109 (2011).

<sup>24</sup>A. Meyer, R. Dimeo, P. Gehring, and D. Neumann, *Rev. Sci. Instrum.* **74**, 2759 (2003).

<sup>25</sup>R. Aзуаh, L. Kneller, Y. Qiu, P. L. W. Tregenna-Piggott, C. Brown, J. Copley, and R. J. Dimeo, *J. Res. Natl. Inst. Stand. Technol.* **114**, 341 (2009).

<sup>26</sup>J. Teixeira, M.-C. Bellissent-Funel, S. H. Chen, and A. J. Dianoux, *Phys. Rev. A* **31**, 1913 (1985).

<sup>27</sup>W. S. Price, H. Ide, and Y. Arata, *J. Phys. Chem. A* **103**, 448 (1999).

<sup>28</sup>Z. N. Buck, A. Miskowiec, A. Mazza, J. Schaeperkoetter, H. Kaiser, F. Y. Hansen, Z. Lemon, and H. Taub, "Neutron diffraction investigation of the structure of ice in proximity to single-supported DMPC and DMPG membranes" (unpublished).

<sup>29</sup>T. J. Zwang, W. R. Fletcher, T. J. Lane, and M. S. Johal, *Langmuir* **26**, 4598 (2010).

<sup>30</sup>C. Faure, L. Bonakdar, and E. J. Dufourc, *FEBS Lett.* **405**, 263 (1997).